

Letters to ESEX

The use of RFID in soil-erosion research

Anthony John Parsons,^{1*} Yuichi Onda,² Takehiro Noguchi,² Jeremy Patin,³ James Cooper,⁴ John Wainwright⁵ and Naoki Sakai⁶

¹ Department of Geography, University of Sheffield, Sheffield, UK

² Centre for Research in Isotopes and Environmental Dynamics, University of Tsukuba, Tsukuba, Ibaraki, Japan

³ Graduate School of Life and Environmental Sciences, Integrative Environmental Sciences, University of Tsukuba, Tsukuba, Japan

⁴ School of Environmental Sciences, University of Liverpool, Liverpool, UK

⁵ Department of Geography, Science Laboratories, University of Durham, Durham, UK

⁶ National Institute for Earth Science and Disaster Prevention, Earth Science and Disaster Prevention, Tsukuba, Japan

Received 10 June 2014; Revised 17 July 2014; Accepted 17 July 2014

*Correspondence to: Anthony John Parsons, Department of Geography, University of Sheffield, Winter Street, Sheffield, S10 2TN, UK. E-mail: a.j.parsons@sheffield.ac.uk

ESPL

Earth Surface Processes and Landforms

ABSTRACT: In this paper, we examine the use of radio frequency identification (RFID) tags for studying soil erosion. Surrogate soil particles were created by coating RFID tags with silicone clay and bronze powder to give them an overall density similar to that of quartz particles. The particles were between 2.5 mm and 4.0 mm in diameter and had specific weights of 2.5 to 3.0. These tagged particles were deployed on two plots: first, in a proof-of-concept laboratory study and secondly in a field study, the latter involving repeated surveys after rainfall events. Seven surveys under natural rainfall over four months yielded recovery rates averaged 56%. RFIDs are shown to provide useful insights into the movement of individual soil particles during erosion processes. As RFID technology advances, further miniaturization is likely to occur enabling the movement of a greater range of soil particles to be studied, and we may anticipate improvements to the signal detection so that recovery does not rely wholly on visual identification. Copyright © 2014 John Wiley & Sons, Ltd.

KEYWORDS: soil erosion; particle tracking; radio-frequency identification

Introduction

The processes of soil erosion occur at the scale of the individual soil particle (Cooper *et al.*, 2012). However, understanding of the movement of individual soil particles during the erosion process is difficult to obtain, largely because of the size of soil particles. Whereas studies of bedload transport in rivers have been able to trace the movement of individual clasts over single flood events (e.g. Hassan *et al.*, 1984, 1992), such detailed understanding has largely eluded the field of soil erosion. Much previous work in which tracers have been used to study soil erosion has been directed at using such tracers to obtain rates of soil erosion, rather than information on the movement of individual soil particles (for a review of such techniques, see Guzman *et al.*, 2013). Where tagging of particles has been used to examine the movement of individual soil particles, bulk tags have generally been limited to providing a distribution of the movement of the particles (e.g. Parsons *et al.*, 1993; Furbish *et al.*, 2007; Armstrong *et al.*, 2012; Darvishan *et al.*, 2013). Although Poesen *et al.* (1997) did measure the movement of individually labelled, tagged particles, these particles were 0.015 m in diameter and simulated the movement of rock fragments within the soil rather than the soil itself. Two new technologies [particle imaging velocimetry (see Long *et al.*, 2014) and radio frequency identification (RFID)], however, offer the possibility of tracking the movement of individual eroded soil particles. Here we examine the use of RFID for studying soil erosion.

Methodology

A RFID tag is a tiny integrated circuit chip (Figure 1a). Each tag has an individual ID number. The RFID tag used in this study was made by TOPPAN FORMS Co., Ltd, Japan, and has a size of 2 mm × 1.8 mm × 0.4 mm. The tags are read by using R/W (TOPPAN FORMS Co., Ltd, Figure 1b).

In order to use RFID tags for soil-erosion research they need to be made similar to soil particles. As manufactured, the tags are plate-like and less dense than soil particles. For this study the RFID tags were coated in a clear silicone resin (Nisshin Associates Co., Ltd, Japan), in order to make them roughly spherical in shape, and then coated in bronze powder to give them an overall density similar to that of quartz particles. For ease of identification, they were further coated in fluorescent powder. The final surrogate soil particles were between 2.5 mm and 4.0 mm in diameter and had specific weights of 2.5 to 3.0. As each particle was made by hand the size and specific weights vary. These tagged particles were deployed on two plots: first, in a proof-of-concept laboratory study and secondly in a field study.

Laboratory plot

The laboratory study was conducted using the large-scale rainfall simulator at the National Research Institute for Earth Science and Disaster Prevention (NIED), Tsukuba, Japan. The

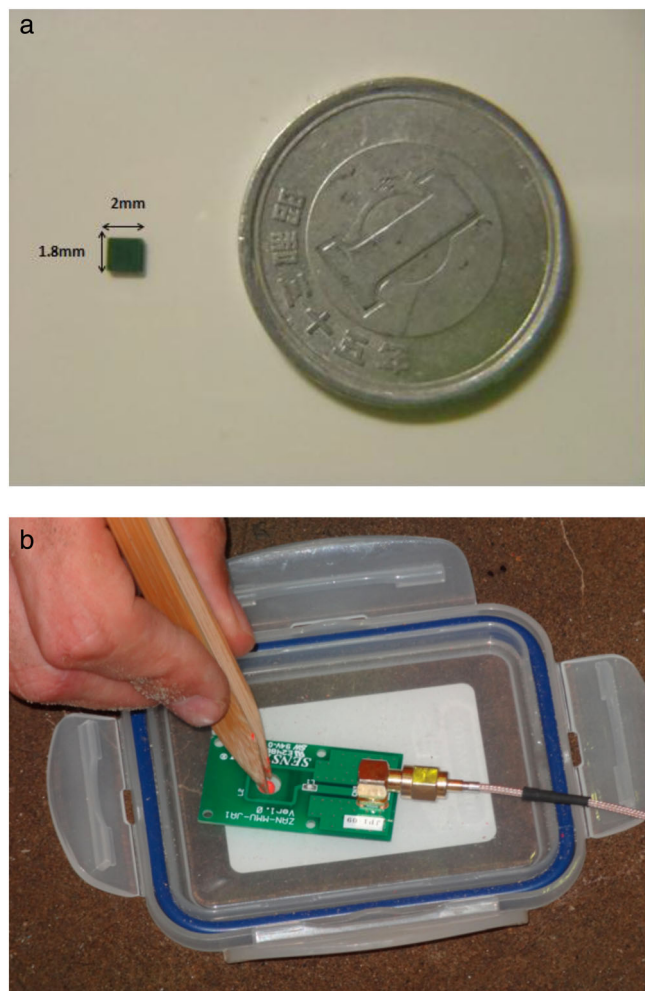


Figure 1. (a) The RFID tag embedded into the manufactured 'soil' particles. One-Yen coin for scale. (b) The RFID reader. This figure is available in colour online at wileyonlinelibrary.com/journal/espl

plot was 1 m wide \times 4.8 m long and had a gradient of 3°. One hundred RFID particles were placed on the soil surface of this plot in a 300 mm \times 300-mm array of uniformly spaced particles located midway across the plot and centred 3.6 m from the upper boundary. A rainfall simulation lasting 15 minutes was conducted on this plot at an intensity of 60 mm h⁻¹. This experiment was short enough that no runoff occurred and that all particle movement was a result of raindrop impact. Prior to and after the experiment the locations of the tags were surveyed *in situ* using a laser total station, and the tags were read by the R/W reader (Figure 1b). Because the RFIDs used in this study are passive devices, they can only be read if the reader is in close contact with the tag. Thus the technique is currently limited to visual identification of the particles prior to their being read, if reading is to take place *in situ*. If the experimental design allows removal of particles from the ground surface, excavation can allow recovery of buried particles, the locations of which can be recorded prior to physical removal for reading the tags.

Field plot

The field plot was 5 m wide and 22.13 m long and had a gradient of 4.4°. It was established in a field previously used for tobacco cultivation close to Kawamata, Fukushima Prefecture, Japan (37°35' 53.51"N, 140°40' 25.20"W). The field is now out of cultivation because of the accident at the Fukushima nuclear power plant in 2011. Herbicide was applied to the plot prior to the experiment, so that it was largely free of vegetation.

A sediment trap was installed at the outlet to catch sediment eroded from the plot. A 0.2 mm tipping-bucket rain gauge was installed near the plot, and runoff from the plot was recorded at one-minute intervals. On this plot we located 303 tagged particles. Nine cross-sections located 50 cm, 1 m, 2 m, 3 m, 5 m, 8 m, 11 m, 14 m and 17 m from top of the plot each had 19 tagged particles at 25-cm intervals across the plot (Figure 2). Tagged particles were also located along four profiles down the plot, two of which were in the centre of cultivation furrows and two on cultivation ridges. Thirty-three tagged particles were installed at 0.5-m-intervals along each of these transects starting at 1.0 m from the top of the plot. The location of each tagged particle was recorded using a laser total station at the time of installation (30 June 2012) and at intervals after runoff events until 31 October 2012. Seven resurveys were completed during this period (Table 1; Video S1 in the online supporting information). At each survey, all the sediments were removed from the sediment trap. A terrestrial laser scan of the plot was acquired on 22 October 2012 with a Leica Scanstation C10. The three-dimensional (3D) data was processed and analysed to obtain a digital elevation model of the plot (Figure 2).

Results

Laboratory study

Recovery rate of the RFIDs for the experiment was 97%. Loss of particles is almost certainly due to burial beneath other moving soil; without visual identification the particles are impossible to detect. A further three particles were mislabelled when their locations were recorded. The distribution of the travel distances for the remaining 94 is shown in Figure 3. Resurvey of the four control points at the corners of the array indicates that the error associated with measurement is under 10% of the average transport distance of the particles. Because of this error it is impossible to identify zero movement of an individual particle. Analysis of the distribution of travel distances for the experiment shows that the distribution that does best at fitting the

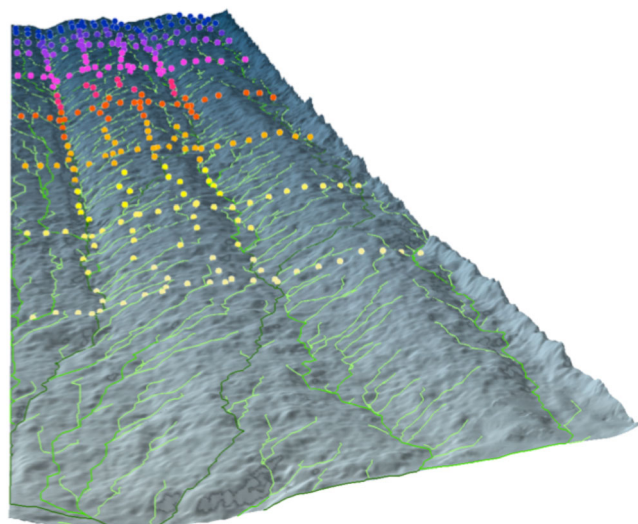


Figure 2. Starting location of RFIDs overlain on a digital elevation model (DEM) of the plot surveyed on 22 October 2012. The DEM is 5.00 m wide, 22.00 m long and has relative elevations from 0.00 m to 1.89 m. RFID colour is based on location along the plot and RFIDs are exaggerated in size to aid visualization. Flow pathways are denoted by the green streamlines calculated in ArcGIS (dark-green lines denote large, green lines denote medium and light-green lines denote small relative contributing areas, respectively). This figure is available in colour online at wileyonlinelibrary.com/journal/espl

Table 1. Surveys of the field plot

Survey date	Number of recovered particles	Percentage loss from previous event	Total rainfall prior to survey (mm)	Total runoff prior to survey (l)	Peak runoff prior to survey (l/min)
20 July	256	15.5	106.0	1705.6	158.6
27 July	207	19.1	78.4	6548.3	268.2
8 September	154	25.6	102.5	3589.3	302.0
30 September	129	16.2	100.5	301.8	105.5
10 October	136	-5.4	48.0	2403.2	138.9
22 October	126	7.4	34.4	n/a	n/a
31 October	134	-6.3	n/a	n/a	n/a

Note: n/a, data not available.

observed travel distances (in terms of its overall performance against the Kolmogorov–Smirnov, Anderson–Darling and Chi-squared goodness-of-fit statistics) is the Dagum 4-parameter distribution (shown fitted on Figure 3). This distribution is one of several heavy-tailed distributions used to model empirical data, and is closely allied to the Burr distribution found by Long *et al.* (2014) to be a good fit for the distribution of travel distances of splashed particles from a single raindrop, though differs from the exponential fits found by Furbish *et al.* (2007) and Ghahramani *et al.* (2012).

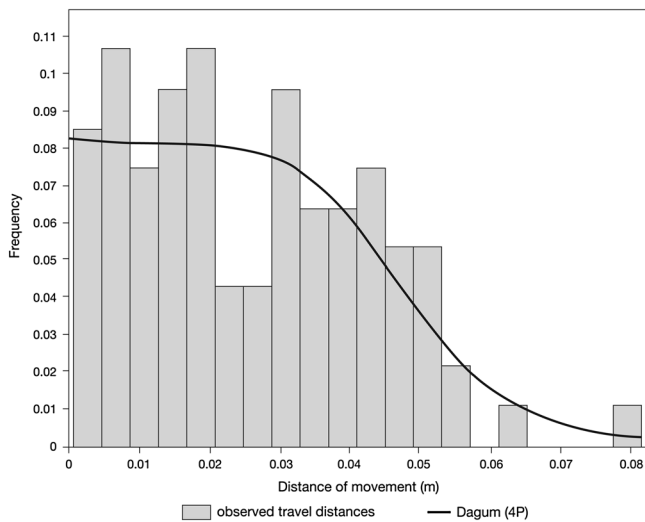


Figure 3. Distributions of travel distance of splashed particles after 15-minute simulated rainstorm at 60 mm h⁻¹ on laboratory plot.

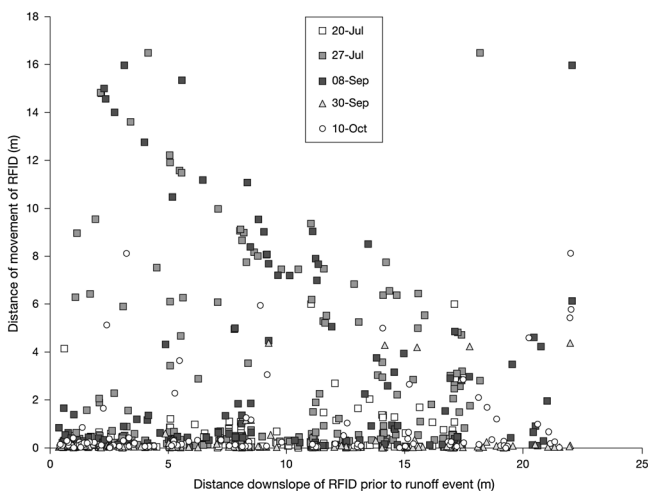


Figure 4. Relationship between distance of movement of RFIDs and location (distance down from the top of the plot) for each survey period.

Field study

Recovery rates for the seven surveys were 85%, 80%, 56%, 42%, 46%, 41% and 44%. As with the laboratory experiments, if RFIDs become buried they are impossible to locate if, as in this case, repeat surveys are planned. These recovery rates include 35 particles that were retrieved from the sediment trap on 27 July (after the largest runoff event). The stability of the number of RFIDs recovered in the four last surveys suggests that by this time burial and re-exposure were balancing out, and may be indicative of recovery rates that can be anticipated for long-term use of RFIDs. Several particles unidentified in one survey were relocated in the next survey.

We have used the data from this plot to examine the effect of distance downslope on travel distance of individual particles to test the hypothesis that as distance downslope (a surrogate for downslope increase in discharge) increases so does travel distance. This hypothesis derives from Parsons *et al.* (1998), who showed that particle travel distance is a function of the product

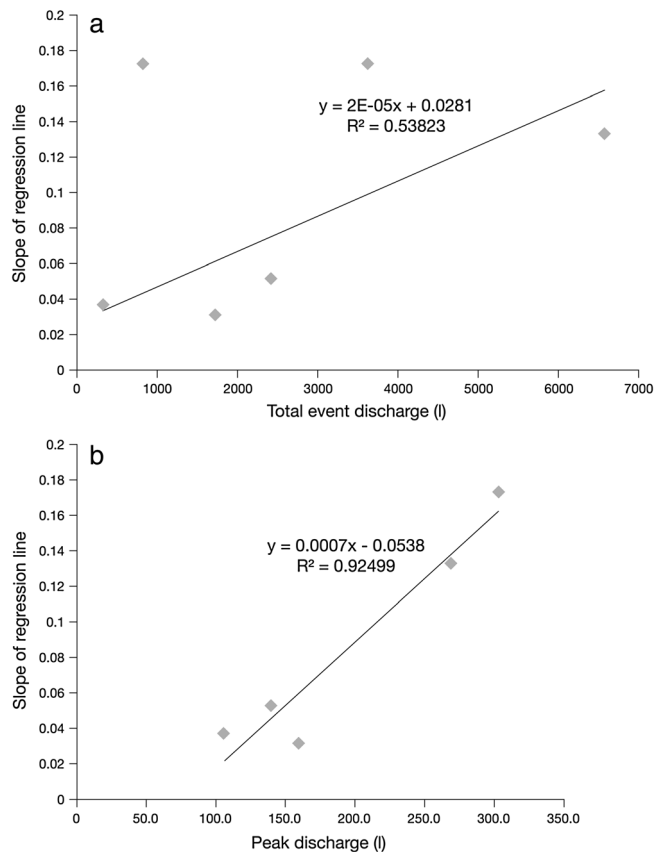


Figure 5. Relationship between rate of change of distance of movement of RFIDs with location and (a) total runoff prior to survey, (b) peak runoff prior to survey.

of rainfall and flow energy. From this work, a linear relationship between travel distance and flow energy would be expected (assuming that rainfall in any given event is spatially uniform over the plot, and that variation in particle mass is spatially random). The data (Figure 4) show very varied travel distances both within and between surveys. As with the laboratory study, no particle shows zero movement, but there is no way to know if very small recorded values of movement are no more than the error associated with the surveying technique. The variability in travel distances is unsurprising, given the likely effects of the plot microtopography (Figure 2) on flow paths and the varied magnitude of the runoff events (Table I; Video S1 in the online supporting information). In order to examine more closely the effects of distance downslope on particle travel distance we have calculated the regression of distance of travel between each survey period on distance downslope, and plotted the slope of these regressions against total and peak discharge recorded in the period prior to each survey (Figure 5) for the five periods for which runoff data are available. These plots reveal remarkably strong correlations. Despite the diverse topographic positions of the individual RFIDs (that contributes to the scatter in Figure 4), the effect of distance downslope on mean travel distance is very strongly related to peak runoff ($R^2 = 0.91$), and this relationship strengthens ($R^2 = 0.97$) if the data from the first survey (at the start of which the RFIDs were lying loose on the surface) are excluded.

Discussion

Both the proof-of-concept laboratory study and the field deployment of the RFIDs have provided insights into the movement of individual soil particles. Under the raindrop-impact process that was investigated in the laboratory, the distance particles move is a function of two probabilities. First, is the probability distribution of particle movement when a group of particles is impacted by an individual raindrop, and the second is the probability of a particle being impacted by a raindrop in a given time period. The study by Long *et al.* (2014) provides information on the former. This study provides the outcome of both probabilities. Detailed analysis of these two types of results should enable the two probabilities to be disentangled. Intuitively, the second probability should be derived from data on rainfall intensity and drop-size distribution. If that proves to be the case, then the data from studies such as that by Long *et al.* (2014) will be more readily integrated into particle-based models of soil erosion, such as that developed by Cooper *et al.* (2012).

Similarly, models of soil erosion based on particle travel distance (e.g. Parsons *et al.*, 2004; Wainwright *et al.*, 2008) have, hitherto, relied upon parameterization derived from laboratory experiments in which the movement of single particles was traced over a rough, fixed bed under conditions of steady rainfall intensities and flow conditions. The field study both confirms the linear relationship between flow energy and travel distance observed in the laboratory experiments, but extends this relationship and indicates that under conditions of unsteady flow and rainfall intensity this linear relationship is most strongly related to maximum flow energy during a storm event.

Conclusion

Our study shows that RFIDs can be used to provide useful insights into the movement of individual soil particles during erosion processes. Such insights are valuable for parameterizing particle-based models of soil erosion (see Cooper *et al.*, 2012) and for testing the predictions of such models. They may also

prove useful for identifying the sources of off-site impacts from soil erosion. At present RFID technology means that simulated soil particles are comparatively large compared to the average size of eroded soil. Nor can they be detected without visual identification. However, as RFID technology advances, further miniaturization is likely to occur enabling the movement of a greater range of soil particles to be studied, and we anticipate improvements to the signal detection (e.g. active tags) so that recovery does not rely wholly on visual identification, and particles can be tracked throughout a rainfall event, providing real-time information on soil erosion dynamics.

Acknowledgement—This research was funded by a grant to Parsons and Onda from the Royal Society under its International Joint Project scheme.

References

- Armstrong A, Quinton JN, Maher BA. 2012. Thermal enhancement of natural magnetism as a tool for tracing eroded soil. *Earth Surface Processes and Landforms* **37**: 1567–1572.
- Cooper JR, Wainwright J, Parsons AJ, Onda Y, Fukuwara T, Obana E, Kitchener B, Long EJ, Hargrave GH. 2012. A new approach for simulating the redistribution of soil particles by water erosion: a marker-in-cell model. *Journal of Geophysical Research - Earth Surface* **117**: F04027. DOI: 10.1029/2012JF002499
- Darvishan KA, Sadeghi SH, Homaei M, Arabkhedi M. 2013. Measuring sheet erosion using synthetic color-contrast aggregates. *Hydrological Processes* **28**: 4463–4471.
- Furbish DJ, Hamner KH, Schmeeckle M, Borusund MN, Mudd SM. 2007. Rain splash of dry sand revealed by high-speed imaging and sticky paper splash targets. *Journal of Geophysical Research* **112**: F01001. DOI: 10.1029/2006JF000498
- Ghahramani A, Yoshiharu I, Mudd SM. 2012. Field experiments containing the probability distribution of particle travel distances during natural rainstorms on different slope gradients. *Earth Surface Processes and Landforms* **37**: 473–485.
- Guzman G, Quinton JN, Nearing MA, Mabit L, Gómez JA. 2013. Sediment tracers in water erosion studies: current approaches and challenges. *Journal of Soils and Sediments* **13**: 816–833.
- Hassan MA, Schick AP, Laronne JB. 1984. The recovery of flood dispersed coarse sediment particles: a three-dimensional magnetic tracing method. *Catena Supplement* **5**: 133–162.
- Hassan MA, Church M, Ashworth PJ. 1992. Virtual rate and mean distance of travel of individual clasts in gravel-bed channels. *Earth Surface Processes and Landforms* **17**: 617–627.
- Long EJ, Hargrave GH, Cooper JR, Kitchener B, Parsons AJ, Hewett C, Wainwright J. 2014. Experimental investigation into the impact of a liquid droplet onto a granular bed using 3D, time-resolved, particle tracking. *Physical Review E* **89**: 032201.
- Parsons AJ, Wainwright J, Abrahams AD. 1993. Tracing sediment movement in interrill overland flow on a semi-arid grassland hillslope using magnetic susceptibility. *Earth Surface Processes and Landforms* **18**: 721–732.
- Parsons AJ, Stromberg SGL, Greener M. 1998. Sediment-transport competence of rain-impacted interrill overland flow. *Earth Surface Processes and Landforms* **23**: 365–375.
- Parsons AJ, Wainwright J, Powell DM, Kaduk J, Brazier RE. 2004. A conceptual model for determining soil erosion by water. *Earth Surface Processes and Landforms* **29**: 1293–1302.
- Poesen J, van Wesemael B, Govers G, Martinez-Fernandez J, Desment P, Vandaele K, Quine T, Degraer G. 1997. Patterns of rock fragment cover generated by tillage erosion. *Geomorphology* **18**: 183–197.
- Wainwright J, Parsons AJ, Mueller E, Brazier R, Powell DM, Fenti B. 2008. A transport-distance approach to scaling erosion rates: 1. Background and model development. *Earth Surface Processes and Landforms* **33**: 813–826.

Supporting Information

Additional supporting information may be found in the online version of this article at the publisher's web site.